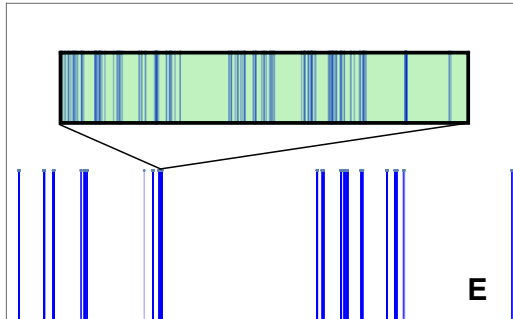


Random Cantor sets and mini-bands in local spectrum of quantum systems

B. L. Altshuler, V. E. Kravtsov



Highlights

Random Cantor sets and mini-bands in local spectrum of quantum systems

B. L. Altshuler, V. E. Kravtsov

- Non-ergodic extended states and a singular-continuous (s.c.) spectrum
- Two types of s.c. spectrum: Cantor set and isolated mini-band
- Model for s.c. spectrum: i.i.d. power-law spacing distribution
- Correlation function of LDoS $K(\omega)$ as a measure for s.c. spectrum
- Singularity of $K(\omega)$ at $\omega = 0$ for s.c. spectrum in the infinite system

Random Cantor sets and mini-bands in local spectrum of quantum systems

B. L. Altshuler^a, V. E. Kravtsov^b

^a*Department of Physics, Columbia University, 116th and Broadway, New York, 10027, NY, U.S.A.*

^b*The Abdus Salam International Centre for Theoretical Physics, P.O.B. 586, Trieste, 34100, Italy*

Abstract

In this paper we give a physically transparent picture of singular-continuous spectrum in disordered systems which possess a non-ergodic extended phase. We present a simple model of identically and independently distributed level spacing in the spectrum of local density of states and show how a fat tail appears in this distribution at the broad distribution of eigenfunction amplitudes. For the model with a power-law local spacing distribution we derive the correlation function $K(\omega)$ of the local density of states and show that depending on the relation between the eigenfunction fractal dimension D_2 and the spectral fractal dimension D_s encoded in the power-law spacing distribution, a singular continuous spectrum of a random Cantor set or that of an isolated mini-band may appear. In the limit of an infinite number of degrees of freedom the function $K(\omega)$ in the non-ergodic extended phase is singular at $\omega = 0$ with the branch-cut singularity for the case of a random Cantor set and with the δ -function singularity for the case of an isolated mini-band. For an absolutely continuous spectrum $K(\omega)$ tends to a finite limit as $\omega \rightarrow 0$. For an arbitrary local spacing distribution function we formulated a criterion of fractality of local spectrum and tested it on simple examples.

Keywords: non-ergodic extended states, multifractality of wave functions, singular-continuous spectrum, Cantor set, mini-bands

1. Preamble

This paper is dedicated to memory of our friend, collaborator and teacher Kostya Efetov. His scientific fearlessness, persistent innovation and human

qualities made an unforgettable and crucial impact on our scientific careers, as well as on the development of our scientific community as a whole.

2. Introduction

Recently there has been a vigorous discussion on the existence of *non-ergodic extended (NEE) states* in a finite range of parameters (*NEE phase*) of various disordered systems, both free-particle [1, 2, 3, 4, 5, 6, 7, 8, 9, 10] and interacting [11, 12, 13, 14, 15, 16, 17, 18, 19]. By *extended* states one denotes the states that occupy an extensive part of the Hilbert space, while the lack of ergodicity implies that not all the Hilbert space is occupied by a wave function. The most well-known example of such NEE states are the multifractal states at the critical point of the Anderson localization transition [20]. They, however, do not form a *phase*. Another example of such states are the states in the Critical Power-Law Banded Random Matrices [21] which can be viewed as a one-dimensional systems with long-range hopping. In this case, however, all the states have an NEE, multifractal character. The first and the simplest system which possesses the NEE phase separated by the *ergodic transition* from the ergodic states and by the Anderson *localization transition* from the localized states was found in the generalized Gaussian Rosenzweig-Porter (RP) model [22, 3] and further elaborated in [4, 7, 23] to finally bring it to the status of a mathematical theorem [5].

Remarkably, in Ref.[4] the question of the structure of the local spectrum in the Rosenzweig-Porter model was raised and it was shown that this spectrum has a non-trivial form of a *mini-band*. This peculiarity of the spectrum determines the local dynamics of this model, e.g. the return, or survival, probability, which was studied in detail in Ref.[24]. Furthermore, a modification of the RP model, the log-normal RP model [7], was shown [25] to exhibit a *sub-difusive*, stretch-exponential relaxation of the averaged survival probability, similar to that in the extended phase of the Anderson localization model on a Random Regular Graph [26, 27] and in interacting spin-chains [28, 29, 30, 31, 32, 33, 13]. Since the character of local spectrum determines local dynamics and the latter is important for manipulation of the chains of qubits (which are equivalent to interacting spin-chains), the problem of local spectra has a wide application in quantum computing.

There is, however, another, fundamental dimension in this problem. From the mathematical literature [34] it is known that the spectrum of any Hamiltonian can be decomposed into a sum of three distinctly different types

of spectra: the pure-point, absolutely continuous and singular-continuous. Their loose definitions are the following:

- **(a) pure point:** This type of spectrum corresponds to L^2 integrable *eigenfunctions*, e.g. the *localized* wave functions with a finite localization radius. Finite-amplitude delocalized wave functions (e.g. the plane waves) and those localized in one single point [e.g. $\psi \sim \delta(p - p_0)$ in the momentum space] are not L^2 -integrable in an infinite continuous system and, therefore, they cannot correspond to a pure point spectrum according to the mathematical literature. By *spectrum* we understand the set of real numbers $\{E_n\}$ such that the operator $\hat{H} - E_n$ is not invertible.
- **(b) absolutely-continuous:** In this case the wave functions are *not* L^2 integrable (not normalizable). These maybe the delocalized wave functions in an infinite coordinate space, or the corresponding non-normalizable in the continuous space functions divergent strongly enough at some point p in the momentum space. For this type of spectrum the set of E_n must be *dense*, i.e. for any given real E inside the spectrum there is a E_n such that $|E - E_n|$ is arbitrary small.
- **(c) singular-continuous:** Loosely speaking, this is the type of spectrum that does not fall in neither of the above two types (a) and (b). This means that the corresponding wave functions are *extended* in some basis (otherwise they belong to (a)) but the set of E_n is *not dense*. The archetypical example of such a spectrum is the regular Cantor set. Indeed, in the Cantor set there is a hierarchy of gaps (nearest neighbor spacings) $\delta_m = 3^{-m}$ ($m = 1, 2, \dots, \ln N / \ln 3$) which values in the limit $1/N \rightarrow 0$ are accumulated near $\delta_\infty = 0$. Therefore any point E inside such a spectrum falls inside some gap δ_n with a fixed *finite* n which does not shrink to zero as $1/N \rightarrow 0$. Instead, with increasing N more small gaps of the higher generations $m \gg n$ appear and accumulate near $\delta_\infty = 0$. Hence, the distance $|E - E_n|$ with $E \in \delta_n$ remains finite in this limit, and the spectrum is *nowhere dense* albeit contains an infinite number $N \rightarrow \infty$ of levels.

The above definitions make sense in the continuous systems, while the most of physical systems are defined on discrete sites of some lattices or graphs. In such systems at an infinite number of sites N the non-normalizability can

happen only for extended wave functions, while any localized wave function is always normalizable. However, the Fourier transform of the extended wave function is a localized one and vice versa. Thus the normalizability in the infinite discrete systems is not basis-invariant, while the global spectrum is. This means that normalizability in discrete systems cannot be used for classification of basis-invariant global spectra like in the above definitions for the continuous systems.

However, even in discrete systems one may classify the spectra but in a non-invariant way associated with a certain basis. In order to accomplish this goal we consider the *local density of states* (LDoS) and its correlation functions where the spectral δ -functions $\delta(E - E_n)$ are weighted by the amplitudes $|\psi_n(r)|^2$ of the *normalized* eigenfunctions at a position r in a chosen basis. However, if one adopts this route one should inevitably consider a finite dimension of the Hilbert space N , as otherwise the amplitude of an *extended* eigenfunction will be zero. In such a discrete finite- N systems the spectrum is always discrete and the solutions $\psi_n(r)$ of the Schrodinger equation are always normalizable. The limit $N \rightarrow \infty$ should be implemented only in the final results for the correlation functions of the LDoS.

The question is: Which are the analogues of the pure point, absolutely continuous and singular continuous for the *local* spectra (e.g. the spectra seen in LDoS) and how to distinguish statistically between them? The simple solution we propose is to study the behavior of the local density of states correlation function $K(\omega)$ in the limit $N \rightarrow \infty$, where ω is the difference in the energy. We show that for a local analogue of the absolutely continuous spectrum (referred to as *l-absolutely continuous spectrum*) this correlation function has a finite limit at $\omega \rightarrow 0$, while for the *l-singular continuous spectrum* $K(\omega)$ is singular at $\omega = 0$. For a *l-pure point spectrum* $K(\omega \rightarrow 0) = 0$, the limit $N \rightarrow \infty$ should be taken first in all three cases.

A crucial step in doing this limit is to discriminate eigenstates according to their amplitude at the observation point r and eliminate the states which amplitude $|\psi_i(r)|^2$ is lower than the discriminant level $\sim 1/N$. In the non-ergodic phases, this operation diminishes drastically the number of states remaining in the spectrum of LDoS (the "local levels") and it also changes qualitatively statistics of spacing between the corresponding energy levels leading to the fat tails in the level spacing distribution.

We propose the following classification of the local spectra:

- *l-pure point spectrum (a)*: This type of local spectrum emerges in the

localized systems. The local spectrum consists of a finite number of levels with the typical spacing that remains finite as $N \rightarrow \infty$. The corresponding states are all localized in the same localization volume.

- *l-absolutely continuous spectrum (b)*: The local spectrum is dense in the limit $N \rightarrow \infty$ in a certain spectral interval that remains finite in this limit. This type of spectrum corresponds to the *ergodic delocalized states*.
- *l-singular continuous spectrum (c)*: These are the local spectra that do not fall in neither of the above types (a) and (b). Two important examples are: **(i)** The local spectrum contains an infinite number of levels in a certain finite interval of energies in the limit $N \rightarrow \infty$. However, the spectrum is not dense in this interval (e.g. it is a random Cantor set). Alternatively, **(ii)** the local spectrum is all concentrated within a *mini-band* that contains an infinite number of levels in the $N \rightarrow \infty$ limit but the width of the mini-band shrinks to zero in this limit.

We will show below that in the case **(i)** $K(\omega) \sim \omega^{-\alpha}$, $0 < \alpha < 1$ in the limit $N \rightarrow \infty$, while in the case **(ii)** $K(\omega) \sim \delta(\omega)$ in this limit.

In order to substantiate this classification we consider a simple model of local levels with independent identically distributed (i.i.d.) spacing which distribution is a power-law. We show that such a simple model is capable of reproducing the two principle cases of *l-singular continuous spectra*: the random Cantor set and the isolated mini-band. We show that upon a proper choice of parameters such a model gives a correct behavior of $K(\omega)$ both for the Power-Law Banded Random Matrices and for the Gaussian Rosenzweig-Porter random matrix ensemble. This allows us to conclude that the local spectrum of the former is a random Cantor set, while that of the latter is an isolated mini-band with the dense spectrum inside a mini-band.

However, our model gives many more possibilities of singular continuous spectra which Hamiltonian realizations are not yet found. Thus it can be viewed as a guide for a further search of such models.

Finally, we extend our model of i.i.d. local spacings to an it arbitrary distribution of spacings and formulate a general criterion of fractality of local spectrum. This criterion may be used to characterize complex statistics of local spectra in random systems.

The paper is organized as follows. In Introduction (Section 2) we review the relevant literature and discuss the difference between the classification

of global spectra in continuous systems in mathematical literature and classification of local spectra in discrete systems in this work. In Section 3 we describe the procedure of discrimination of eigenstates which explains a qualitative difference between the global and the local spectral statistics. The two principle classes of the l -singular continuous spectra and the corresponding Hamiltonian realizations are also described in this section. In Section 4 a toy model of local spectrum of the form of the textbook Cantor set is considered, the power-law spacing distribution $P(s)$ in this model is derived and the model local density of states correlation function $K(\omega)$ is computed. In Section 5 a random Cantor set is constructed from the i.i.d. power-law local spacing distributions and the correlation function $K(\omega)$ is computed. In Section 6 from the same model of i.i.d. local spacing distributions we obtain an isolated mini-band. In Section 7 a general criterion of fractality of local spectrum is formulated for an arbitrary $P(s)$. This formalism is tested in Appendix A for a power-law $P(s)$ for a choice of parameters that corresponds to a random Cantor set and to an isolated mini-band in the NEE phases and to a dense spectrum in ergodic phases. In Conclusion we present the table of all the principle results for the ω - and N - dependence of the local DoS correlation function $K(\omega)$ and for the scaling of the mini-band with the dimension N of the Hilbert space. Finally, in Conclusion we present an expression for $K(\omega)$ in $N \rightarrow \infty$ limit which distinguishes between the absolutely continuous and the two principal classes of the singular continuous spectra that emerge in our model.

3. Discrimination of eigenstates

3.1. The global and the local density of states

We start by reviewing the differences between the global and the local spectrum of a quantum system with the broad distribution of the eigenfunction amplitudes $|\psi_n(r)|^2$. In this section we introduce the notion of a mini-band in the local spectrum and the peculiarities of the local spacing distribution compared to its global counterpart.

First of all we remind the readers the definitions of the global, $\rho(E)$, and the local, $\rho(E; r)$, densities of states (DoS) in terms of the eigenvalues E_n and eigenfunctions $\psi_n(r)$:

$$\rho(E) = \frac{1}{N} \sum_n \delta(E - E_n), \quad (1)$$

$$\rho(E; r) = \sum_n |\psi_n(r)|^2 \delta(E - E_n). \quad (2)$$

In disordered systems both $\rho(E)$ and $\rho(E; r)$ are random quantities. By normalization of the eigenfunctions:

$$\sum_r |\psi_n(r)|^2 = 1, \quad (3)$$

the mean eigenfunction amplitude is given by:

$$\langle |\psi_n(r)|^2 \rangle = N^{-1}, \quad (4)$$

where $\langle \dots \rangle$ denotes the ensemble average and N is the dimension of the Hilbert space (the total number of eigenfunctions).

If the distribution of the eigenfunction amplitudes is narrow $|\psi_n(r)| \sim N^{-1}$ (as it happens e.g. for the Wigner-Dyson random matrices) then there is no qualitative difference between the statistics of the global and the local DoS. On the other hand, for the localized eigenfunctions only few of them have an appreciable amplitude in the observation point r . If one discards the states with exponentially small amplitudes in the observation point, the local spectrum will consist of a finite number of the δ -functions with a finite separations between them in the thermodynamic limit $N \rightarrow \infty$ (an l -pure point spectrum). In contrast, the global spectrum in most of the cases has a dense set of eigenvalues with the mean level spacing $\delta \sim N^{-1}$ that vanishes in the limit $N \rightarrow \infty$. In what follows we will always assume that the global spectrum is *dense*, i.e. in the thermodynamic limit in the arbitrary close vicinity ϵ of any point E inside the spectral band there is an eigenvalue E_n such that $|E - E_n| < \epsilon$.

The two limiting examples mentioned above: (i) the absolutely continuous local and global spectra of the Wigner-Dyson random matrices [35] and (ii) the pure point local spectrum concomitant with absolutely continuous global spectrum of localized eigenstates, do not cover all the possible cases. Below we describe other possibilities of the *l-singular continuous spectra* and present a transparent physical picture as to why and where they may arise.

3.2. Discrimination of eigenstates and the fat tail in the local level spacing distribution

The main cause for a drastic difference between the statistics of the local and the global spectrum is best illustrated by the example of the localized

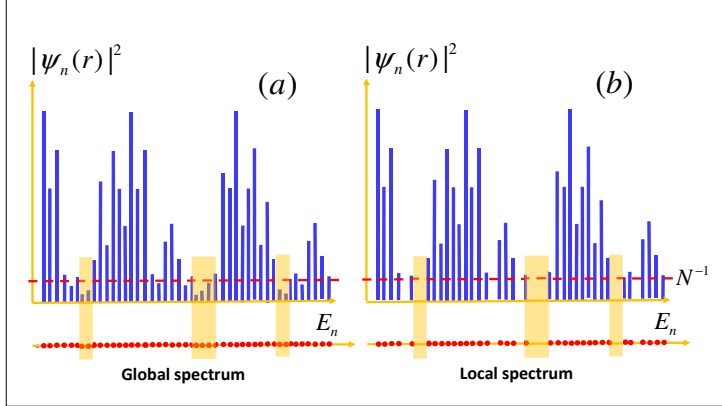


Figure 1: (Color online) Eigenstates before (a) and after (b) discarding states with the amplitude at the observation point r smaller than the discrimination level $\sim N^{-1}$ (red dashed lines). As the result of discrimination large gaps appear in the local spectrum (e.g. in the yellow shadowed areas).

eigenstates. It is the *broad distribution* of the eigenfunction amplitudes. In the case of localized eigenstates there are rare large amplitudes if the localization center is close to the observation point and the range of exponentially small amplitudes if the observation point is beyond the localization volume. This allows to introduce a *discriminant* such that the eigenstates with amplitudes smaller than the discriminant level are discarded from the local spectrum (see Fig.1). In practice the discriminant level should be chosen to be much lower than the mean eigenfunction amplitude $\langle |\psi_n(r)|^2 \rangle = N^{-1}$. The obvious consequence of that is the emergence in the local spectrum of level spacings much larger than those in the global one (see Fig.1). Statistically, this exhibits itself in the fat tails in the local spacing distribution function.

An important special case is when *after the discrimination* the number of states in the local spectrum M is infinite in the thermodynamic limit but it scales with N like a fractional power of N :

$$M \sim N^{D_s}, \quad 0 < D_s < 1 \quad (5)$$

In this case the mean level spacing δ_{av} in the local spectrum scales like $M^{-1} \sim N^{-D_s}$, while the typical level spacing $\delta_{\text{typ}} \sim \delta$ is supposed to be the same as

in the global one ¹:

$$\delta_{\text{typ}} \approx \delta = 1/N, \quad \delta_{\text{av}} \sim N^{-D_s}. \quad (6)$$

Here and everywhere throughout the paper we assume that the energy units are chosen so that the global spectral band-width is equal to 1.

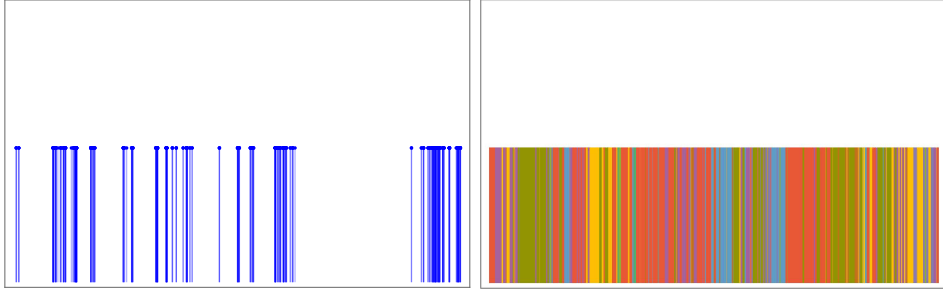


Figure 2: (Color online) (Left panel): Random Cantor set in the local spectrum with $D_s = 0.63$. (Right panel): Dense global spectrum as a unification of random Cantor sets (shown by different colors) seen in different observation points.

3.3. Random Cantor set in Power-Law banded random matrices

A well-known example of such a situation is a random Cantor set (see Fig.2) which will be considered in detail in the next Section. This type of local spectrum is realized in the Critical Power-Law Banded Random Matrix (CPLBRM) ensemble [21] defined as follows. It is an ensemble of random Hermitean matrices \hat{H} with real or complex entries $H_{nm} = \Re H_{nm} + i\Im H_{nm}$ with statistically independent real and imaginary parts, $\Re H_{nm} = \Re H_{mn}$ and $\Im H_{nm} = -\Im H_{mn}$, which are the Gaussian distributed random variables with zero mean and the variance:

$$\langle |H_{nm}|^2 \rangle = \frac{1}{1 + (n - m)^2/b^2}, \quad (7)$$

where the only control parameter is the band-width $0 < b < \infty$. It is well-known [20] that all eigenstates $\psi_i(r)$ of such matrices are multifractal, i.e.

¹In general, the discrimination procedure insures only that $\delta_{\text{typ}} \gtrsim \delta$. However, it seems natural that for the extended states the amplitudes are correlated at a scale of δ . Therefore if a state survives the discrimination, the neighboring in energy state is likely to do so.

they are extended but non-ergodic with

$$\sum_r |\psi_i(r)|^{2q} \sim N^{-D_q(q-1)}, \quad (8)$$

where the q -dependent $0 < D_q < 1$ is the eigenfunction multifractal dimension that varies from 0 to 1 as the parameter b increases from $b = 0$ to $b = \infty$.

3.4. Mini-bands in the local spectrum: Rosenzweig-Porter Random matrix ensemble

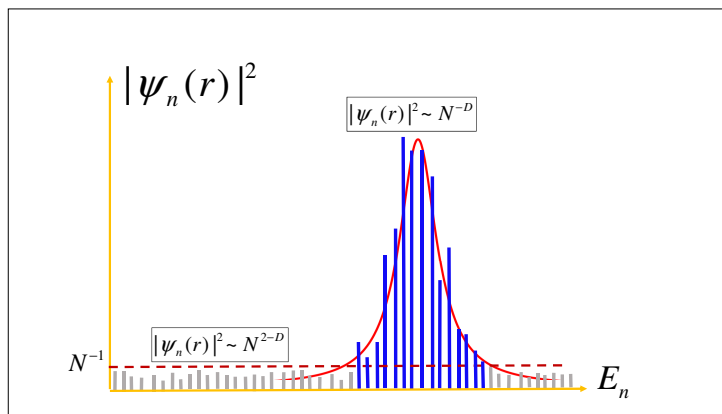


Figure 3: (Color online) Typical local spectrum of the Rosenzweig-Porter random matrix ensemble in its non-ergodic extended phase. States depicted in blue survive discrimination (set by the red dashed line) and form a mini-band with the Lorentz envelope of $|\psi_n(r)|^2$ (red solid line). The states shown in gray are discarded. The number of levels in the mini-band $M \sim N^D$ is extensive but at $0 < D < 1$ is much less than the total number of states N . The width of the Lorentzian envelope is $M\delta \sim N^{-(1-D)}$ and tends to zero in the thermodynamic limit.

The difference between the global and the local DoS in the delocalized systems is especially drastic when most of the states are discarded in the discrimination process and the remaining ones form a compact *mini-band* (see Fig.3). Such a situation emerges in the Rosenzweig-Porter (RP) random

matrix ensemble [22, 3, 4, 36, 23]. As in the case of CPLBRM the RP random matrices have statistically-independent random Gaussian entries with zero mean. But the variance is bi-modal:

$$\langle |H_{nn}|^2 \rangle = 1, \quad \langle |H_{n \neq m}|^2 \rangle = N^{-\gamma}, \quad (9)$$

where $0 < \gamma < \infty$ is the effective disorder parameter, and N is the size of a matrix.

In the non-ergodic extended phase $1 < \gamma < 2$ the mini-band in this model contains $M \sim N^D$ fractal states of the typical amplitude $|\psi|^2 \sim N^{-D}$ characterized by the fractal dimension:

$$D_q = D = 2 - \gamma, \quad (10)$$

which is independent of q for all $q > 1/2$. It is important that inside the mini-band the statistics of local spectrum is Wigner-Dyson [35, 37, 24, 38]. Thus in the thermodynamic limit $N \rightarrow \infty$ the width of the mini-band $M\delta \sim N^{D-1}$ shrinks to zero but the number of levels in it tends to infinity.

4. Regular Cantor set as a spectral counting function

In order to better understand the properties of the random Cantor set and its connection with the local spectrum of quantum systems such as CPLBRM, let us consider the toy model of local spectrum in a form of a regular textbook Cantor set. Namely, let us consider a set of $M = N^{D_s}$ delta-functions $\delta(E - E_n)$ with the equal weight $|\psi_n(r)|^2 = N^{-D_s}$. Such a model obeys the completeness condition:

$$\sum_{n=1}^M |\psi_n(r)|^2 = 1. \quad (11)$$

The points E_n in the segment $[0, 1]$ which represent the eigenvalues in this toy model are organized in generations as follows (see Eq.(12)). The first generation consists of two points $1/3$ and $2/3$ which are the ends of the central $1/3$ -segment. The second generation are the ends of the central $1/3$ -segment of the remaining two segments. This procedure is repeated until the minimal spacing 3^{-n} becomes N^{-1} .

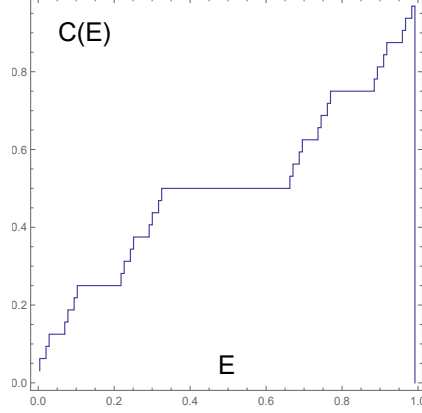


Figure 4: (Color online) Cantor counting function

4.1. Construction of a regular Cantor counting function

Now let us construct the *counting function* $C(E)$ corresponding to the regular Cantor set defined by Eq.(12):

$$C(E) = M^{-1} \sum_{i=1}^M \theta(E - E_i), \quad (17)$$

where $\theta(x)$ is the Heaviside step function, E_i is the ordered set of 'eigenvalues' E_n defined by Eq.(12) and $M \sim N^{D_s}$ is the total number of levels, Eq.(13). The so defined *Cantor counting function* is plotted in Fig.4.

4.2. Convolution of two Cantor counting functions and the LDoS correlation function

From the definition of Cantor counting function it follows that the derivative $\partial_E C(E)$ is the set of δ -functions that mimics the LDoS. For random systems one is interested in the *correlation function* of two LDoS defined by Eq.(2):

$$K(\omega) = \langle \rho(E + \omega/2; r) \rho(E - \omega/2; r) \rangle. \quad (18)$$

In terms of the counting functions:

$$C(E; r) = \sum_n |\psi_n(r)|^2 \theta(E - E_n), \quad (19)$$

we have:

$$K(\omega) = -4 \frac{d^2}{d\omega^2} \langle C(E + \omega/2; r) C(E - \omega/2) \rangle \quad (20)$$

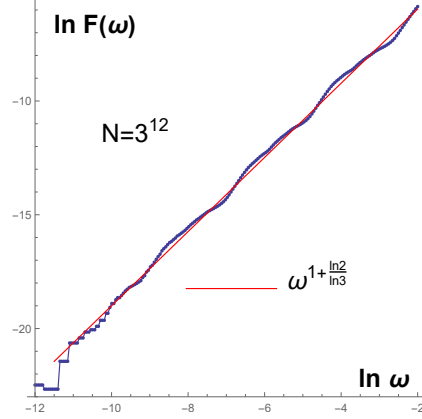


Figure 5: (Color online) $C(E + \omega/2)C(E - \omega/2) - C(E)^2$ integrated over E as in Eq.(21) for the Cantor set with $n = 12$ generations.

In our toy model with the regular Cantor counting function $C(E)$ instead of the random $C(E; r)$ we replace the ensemble averaging by the averaging over the spectrum:

$$K_{\text{Cantor}}(\omega) = -4 \frac{d^2}{d\omega^2} \int_{\frac{\omega}{2}}^{1-\frac{\omega}{2}} C(E + \omega/2)C(E - \omega/2) dE, \quad (21)$$

where $C(E)$ is given by Eq.(17). In Fig.5 the averaging over the spectrum for $F(\omega) = C(E + \omega/2)C(E - \omega/2) - C(E)^2$ is done numerically for the Cantor set with $n = 12$ generations. One can see that the result is well described by a power law $F(\omega) \propto \omega^{1+D_s}$. We conjecture that in the limit $N = 3^n \rightarrow \infty$ this power law becomes exact, so that *down to* $\omega = 0$ we have:

$$K_{\text{Cantor}}(\omega) \propto -4 \frac{d^2 F(\omega)}{d\omega^2} \sim \left(\frac{1}{\omega}\right)^{1-D_s}, \quad \left(D_s = \frac{\ln 2}{\ln 3}\right). \quad (22)$$

The regular Cantor set is the prototype of the *singular continuous spectrum* defined rigorously in mathematical literature [34]. We see, therefore, that the 'smoking gun' of the local analogue of such a spectrum, the l -singular continuous spectrum, in the limit $N \rightarrow \infty$, is the singular behavior of the LDoS correlation function, Eq.(18), at $\omega \rightarrow 0$.

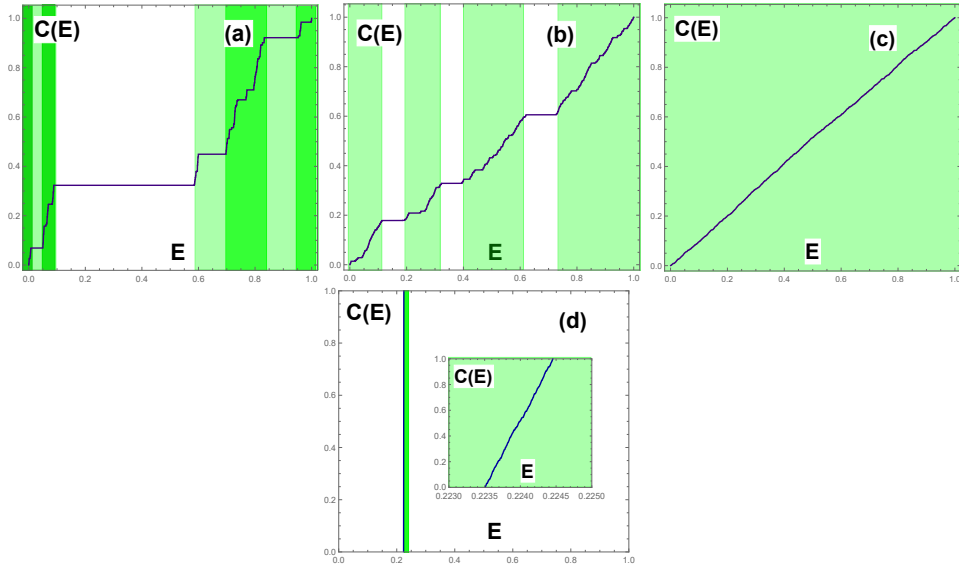


Figure 6: (Color online) The counting function $C(E)$ for a set of $M = N^D$ levels with the power-law spacing distribution, Eq.(16), characterized by: (a) $D = D_s = 0.63$; (b) $D = D_s = 1$; (c) $D = 1, D_s = 2$; (d) $D = 0.5, D_s = 2$. In the random Cantor set (a) the gaps (plateaus) between the mini-bands (green strips) at any scale Δ in the hierarchy (shown by increasing intensity of green strips) are of the order of the typical width of mini-bands. In the case (b) the gaps between the strings of levels shown by green strips, are smaller than the typical width of the strings (a *sub-dense* spectrum). In this case the local spectrum lacks a hierarchy of mini-bands. In the case (c) the spectrum is dense with no large gaps at all. In the case (d) an isolated narrow mini-band appears with the zoomed counting function of the type (c) shown in the inset. A similar isolated mini-band appears in all the cases when $D < D_s$ with the spectrum inside the mini-band being a Cantor set (a) if $D_s < 1$ or it is sub-dense as in (b) if $D_s = 1$.

5. Random Cantor set

5.1. Random Cantor set and its counting function

The power law, Eq.(16) for the spacing distribution in the regular Cantor set can be used to define a *random Cantor set* which is a natural generalization of a regular Cantor set to describe the singular continuous spectrum of random Hamiltonians.

Let us consider a model of local spectrum in which all $s_n = E_{n+1} - E_n$ are:

- independent random quantities,

- distributed identically according to the power-law Eq.(16) with some $1 > D_s > 0$.

An example of the counting function $C(E)$ drawn from such a model of random spectra with $D_s = 0.63$ is shown in Fig.6(a). Like in the regular Cantor set, this counting function consists of the hierarchy of plateaus and staircases between them (denoted by green stripes of increasing intensity as the scale decreases). The length of the staircases (the width of the green stripes) at all scales is of the order of the length of the plateaus at the corresponding scales.

5.2. Correlation function of two random Cantor counting functions

Now we compute the ensemble average of the product of a random Cantor counting function and the same counting function shifted by ω in the energy space. Such an average corresponds to the LDoS correlation function, provided that the local spectrum (after discrimination) is a random Cantor set. We demonstrate that the result of such averaging for a model with $D_s < 1$ reproduces the LDoS correlation function in many critical systems (including the Anderson models at the localization transition and CPLBRM) just corroborating the conjecture that the local spectrum of the corresponding quantum critical systems is a random Cantor set.

Because of independently fluctuating and identically distributed spacings s_j in our model of a random Cantor set one can easily compute the correlation function $K(\omega)$ given by Eq.(20). First we note that since the averaged LDoS and its correlation function $K(\omega)$ for the random Cantor set are independent of E everywhere in the interval $[0, 1]$ one may integrate Eq.(20)[where $C(E; r)$ is given by Eq.(17) with random E_i] over E in this interval and represent $K(\omega)$ as follows:

$$K(\omega) = M^{-2} \sum_{i,i'=1}^M \delta(\omega - E_i + E_{i'}), \quad (23)$$

where $M \leq N$ is the total number of levels E_i in our model of *local* spectrum, and

$$E_i - E_{i'} = \sum_{j=i'}^i s_j. \quad (24)$$

The function $K(\omega)$ is normalized:

$$\int K(\omega) d\omega = 1. \quad (25)$$

Furthermore, for $M \gg 1$ its *regular* part corresponding to $i = i'$ in Eq.(23) also obeys Eq.(25) with the accuracy $O(1/M)$.

Next, using $\langle e^{-i\tau \sum_{j=i'}^i s_j} \rangle = \langle e^{-i\tau s} \rangle^{i-i'}$ that follows from the statistical independence of s_j , and summing the geometric series one obtains for the Fourier transform of $K(\omega)$:

$$\begin{aligned} \tilde{K}(\tau) &= M^{-2} \left[M + 2 \sum_{i'=1}^M \sum_{i=i'+1}^M \Re \langle e^{-i\tau \sum_{j=i'}^i s_j} \rangle \right] \\ &= M^{-1} + 2M^{-2} \Re \left[\left(M - 1 - \frac{g - g^M}{1 - g} \right) \frac{g}{1 - g} \right]. \end{aligned} \quad (26)$$

In Eq.(26) we denote $g \equiv g(t = i\tau)$ where on a real axis $t > 0$:

$$g(t) = \langle e^{-ts} \rangle = \int_0^\infty e^{-ts} P(s) ds. \quad (27)$$

By normalization of the probability distribution $P(s)$ one has on the real axis of t :

$$g(0) = 1, \quad 0 < g(t) \leq 1. \quad (28)$$

The function $\tilde{K}(\tau)$ gives the mean return/survival probability:

$$\tilde{K}(\tau) = \langle |\Psi(\tau; r)|^2 \rangle, \quad (29)$$

where initially at $\tau = 0$ the wave function $\Psi(t = 0, r)$ was non-zero only at a point r .

The spectral form-factor is given by an inverse Fourier transform of $\tilde{K}(\tau)$:

$$K(\omega) = \int_{-\infty}^{+\infty} \tilde{K}(\tau) e^{i\omega\tau} \frac{d\tau}{2\pi}. \quad (30)$$

The function $g(t)$ that corresponds to the distribution Eq.(16) at $0 < D_s < 1$ has a brunch-cut singularity at $t = 0$:

$$g(t) = 1 - c(\bar{t})^{D_s}, \quad (31)$$

where $\bar{t} = t\delta = t/N \ll 1$ and c is a positive constant of order 1. At $D_s = 1$ one obtains:

$$g(t) = 1 + \bar{t} \ln \bar{t}, \quad (32)$$

while for $2 > D_s > 1$ a linear in \bar{t} term appears:

$$g(t) = 1 - c_1 \bar{t} - c_2 \bar{t}^{D_s}. \quad (33)$$

In general a regular \bar{t}^m expansion with an integer m holds for the first $m = [D_s]$ terms, where [...] denotes an integer part.

At large enough M the term $\propto g^M$ in Eq.(26) (i.e. the boundary term in summation of the geometric series) can be omitted. In this case one obtains:

$$\tilde{K}(\tau) \approx 2M^{-1} \Re (1 - g(i\tau))^{-1}, \quad (34)$$

which for a random Cantor set ($D_s < 1$ and $M = N^{D_s}$) results in:

$$K(\omega) \sim \frac{M^{-1} \delta^{-D_s}}{\omega^{1-D_s}} \sim \frac{1}{\omega^{1-D_s}}, \quad (35)$$

i.e. the same power law, Eq.(22), as for the regular Cantor set but with an arbitrary $0 < D_s < 1$.

It is remarkable that Eq.(35) at $D_s = D_2 = d_2/d$ (where d_2 is the multifractal dimension of the critical wave function and d is the dimensionality of the lattice) reproduces exactly the Chalker's ansatz first established by Chalker and Daniel for the Integer Quantum Hall effect at the center of Landau band [39] and later on found true for the d -dimensional Anderson model at the mobility edge $E = E_c$ [40]² and for the Power-Law Banded Random Matrix ensemble [21, 42, 43, 44]. Thus we can argue that in all these cases the local spectrum (after discrimination described in Sec.3) is a random Cantor set.

However, at $D_s = 1$ one obtains from Eqs.(34),(32) a slowly decreasing

$$K(\omega) \sim M^{-1} \delta^{-1} \left(\ln \frac{\omega}{\delta} \right)^{-1}, \quad (36)$$

²The critical region near the mobility edge or the center of Landau band $E = E_c$ is defined so as the critical length $\xi \propto |E - E_c|^{-\nu}$ is larger than the system size $L = N^{\frac{1}{d}}$. Thus in the critical energy window $|E - E_c| < N^{-\frac{1}{\nu d}}$ there are $N^{1-\frac{1}{\nu d}}$ critical states, which by Harris criterion [41] $\nu d > 2$ tends to infinity in the thermodynamic limit.

rather than a constant. Indeed, we see from Fig.6(b) that the corresponding counting function does contain the plateaus and staircases, albeit the length of the staircases is now larger than that of the plateaus. The corresponding local spectrum is no longer a random Cantor set, neither it is dense as for ergodic systems. The model, Eq.(16), with $D_s = 1$ represents a border-line case in between of a random Cantor set and a dense spectrum (which we refer to as a *sub-dense* spectrum). Its Hamiltonian realization is not known so far to the best of our knowledge.

It is only at $D_s > 1$ where the constant $K(\omega)$ at $\omega \gg \delta$ emerges. The point is that with taking the boundary term g^M into account in Eq.(26) one should modify Eq.(34) as follows:

$$\tilde{K}(\tau) \approx 2M^{-1} \Re(1 - g(i\tau) + \eta)^{-1}, \quad (37)$$

where $\eta = M^{-1} \rightarrow +0$.

Then at $D_s > 1$ one obtains from Eq.(33):

$$\tilde{K}(\tau) \sim \Re \frac{M^{-1}}{i\tau\delta + \eta + c_2 (i\tau\delta)^{D_s}}. \quad (38)$$

At $D_s > 1$, in the leading approximation in $\tau\delta \ll 1$ Eq.(38) results in:

$$\tilde{K}(\tau) \sim \Re \frac{M^{-1}}{i\tau\delta + \eta} \rightarrow \pi M^{-1} \delta^{-1} \delta(\tau), \quad (39)$$

which implies a constant

$$K(\omega) \sim M^{-1} \delta^{-1}, \quad (40)$$

at $\omega \gg \delta$, like for a dense local spectrum in the Wigner-Dyson RMT. The corresponding typical counting function is shown in Fig.6(c) and it does not exhibit plateaus which correspond to anomalously large gaps in the local spectrum. This example shows that the case $D_s > 1$ in Eq.(16) is essentially the same as for a fast decreasing $P(s)$ [like the Poisson or the Wigner-Dyson $P(s)$ in the global spectrum] without fat tails. Thus this local spectrum is *dense*, the same as the global spectrum.

6. An isolated mini-band

For a random Cantor set we considered the model in which the number of local levels $M \sim N^{D_s}$, where D_s controls the power-law distribution Eq.(16).

However, this is not the only possibility but a very particular case. Indeed, comparing Eqs.(17) and (19) we see that the number of levels M is in fact related with the multifractal dimension of an eigenfunction. Indeed, in the simplified case (realized in the Rosenzweig-Porter RMT) when all multifractal dimensions $D_q = D$ are identical for $q \geq 1/2$, one may replace, by the order of magnitude, $|\psi_n(r)|^2 \rightarrow N^{-D}$, so that M in Eq.(17) must be $M \sim N^D$ in order to reproduce Eq.(19), while D_s is yet another independent parameter of the model. In a generic multifractal case we have in $K(\omega)$:

$$M \sim N^{D_2}, \quad (41)$$

as the correlation function $K(\omega)$ is second order in $|\psi|^2$.

The question is: What will happen if $D_2 < D_s$? The answer is known for the Rosenzweig-Porter RMT in its fractal phase where $K(\omega)$ has a simple Lorentzian shape [3, 24, 36, 23]. It is nearly independent of ω for $\delta \ll \omega \ll \Gamma$, where $\Gamma \sim N^{-1+D} \gg \delta$ is the width of the mini-band (see Fig.3), and falls down as Γ/ω^2 at $\omega \gg \Gamma$. Can we reproduce this behavior and find the correct scaling of $\Gamma \sim N^{-(1-D)}$ with N from the above model of independently fluctuating spacings with $D_2 < D_s$? As a matter of fact, the answer to this question is affirmative.

Indeed, consider the case $D_2 < D_s$ in Eqs.(41),(16) of our model of independent identically distributed spacings. Then there is a region of ω where $M \ln(g(t \sim 1/\omega)) \lesssim 1$:

$$\begin{aligned} N^{-1+\frac{D_2}{D_s}} \lesssim \omega \ll 1, \quad D_s < 1, \\ N^{-1+D_2} \ln(N^{D_2}) \lesssim \omega \ll 1, \quad D_s = 1, \\ N^{-1+D_2} \lesssim \omega \ll 1, \quad D_s \geq 1. \end{aligned} \quad (42)$$

In this region the boundary term g^M in the summation of geometric series, Eq.(26), cannot be neglected.

A thorough inspection of Eq.(26) in the region Eq.(42) gives the following result:

$$\tilde{K}(\tau) \approx 2 \left(1 - \frac{M}{3} \Re(1 - g(i\tau)) \right). \quad (43)$$

The τ -independent term in Eq.(43) results in a delta-function in ω which corresponds to a fast exponentially decreasing with ω term in the exact $K(\omega)$ which should be neglected in the considered region, Eq.(42). The term proportional to $g(i\tau)$ after Fourier-transforming gives a tail in $K(\omega)$ in the region, Eq.(42), which is proportional to the power-law spacing distribution

$P(s)$:

$$K(\omega) = \frac{2N^{D_2}}{3} P(\omega) \sim \frac{N^{-(D_s-D_2)}}{\omega^{1+D_s}}. \quad (44)$$

For ω smaller than the lower bound of Eq.(42) the boundary term g^M can be neglected and the results, Eqs.(35),(36),(40), of the previous section hold, if one sets $M \sim N^{D_2}$:

$$K(\omega) = \begin{cases} N^{D_s-D_2} \omega^{-(1-D_s)}, & \text{if } D_2 < D_s < 1 \\ N^{1-D_2} \ln^{-1}(\omega/\delta), & \text{if } D_2 < D_s = 1 \\ N^{1-D_2}, & \text{if } D_2 \leq 1, D_s > 1 \end{cases} \quad (45)$$

The function $K(\omega)$ at different relationship between $D_2 \equiv D$ and D_s is plotted in Fig.7.

Eqs. Eq.(44) and (45) show that in order to reproduce the known Lorentzian $K(\omega)$ in the Rosenzweig-Porter RMT one should set $D_s = 1 + \epsilon \equiv 1_+$, where $\epsilon \rightarrow +0$:

$$K(\omega) \sim \begin{cases} N^{1-D_2}, & \delta \ll \omega \ll \Gamma = N^{-(1-D_2)} \\ \frac{N^{-(1-D_2)}}{\omega^2}, & \omega \gg \Gamma = N^{-(1-D_2)} \end{cases}. \quad (46)$$

The constant $K(\omega)$ at $\delta \ll \omega \ll \Gamma$ (see Fig.7(c)) which is similar to that for the Wigner-Dyson RMT, signals of the dense spectrum of levels inside a mini-band (see Fig.3 and the inset in Fig.6(d)). According to our classification presented in Introduction, such type of the spectrum is neither l -pure point, since the number of levels $M \rightarrow \infty$ in the limit $N \rightarrow \infty$, nor it is l -absolutely continuous, as the width of a mini-band $\Gamma \rightarrow 0$ in this limit. The singularity of such a spectrum is corroborated by the fact that in the limit of an infinite system $N \rightarrow \infty$ the correlation function $K(\omega)$, Eq.(46), reduces to a singular $\delta(\omega)$ function.

Remarkably, Eq.(46) reproduces both the behavior of $K(\omega)$ for the Rosenzweig-Porter RMT [3] in all limiting cases and the scaling of the width of a mini-band $\Gamma \sim N^{-(1-D_2)}$ with the system size N . Generalizing this result we conclude from the lower bound in Eq.(42) that the width of a mini-band (seen in $K(\omega)$) in a generic case $D_2 < D_s$ is given by:

$$\Gamma \sim \begin{cases} N^{-1+\frac{D_2}{D_s}}, & \text{if } D_s < 1 \\ N^{-1+D_2} \ln(N^{D_2}), & \text{if } D_s = 1 \\ N^{-1+D_2}, & \text{if } D_s > 1 \end{cases}. \quad (47)$$

Notice that Eq.(44) and (45) do not match at $\omega \sim \Gamma$ if $D_s \geq 1$. This happens because of the narrow interval around $\omega = \Gamma$ of the width $\sim \Gamma N^{-D(D_s-1)} \ll \Gamma$ where a sharp drop of $K(\omega)$ by a factor of $N^{-D(D_s-1)}$ occurs before a power-law tail, Eq.(44), becomes the leading contribution. At large N the amplitude of the power-law tail tends to zero at any $D_s > 1$, so that the edge of a mini-band is sharp on the logarithmic scale. This region of a sharp drop is encoded in the τ -independent term in Eq.(43) and its detailed description is only possible by a full expression, Eq.(26). In Fig.7(c) it is shown that this drop is in fact linear in ω : $K(\omega) \sim N^{1-D} (1 - \omega/\Gamma)$.

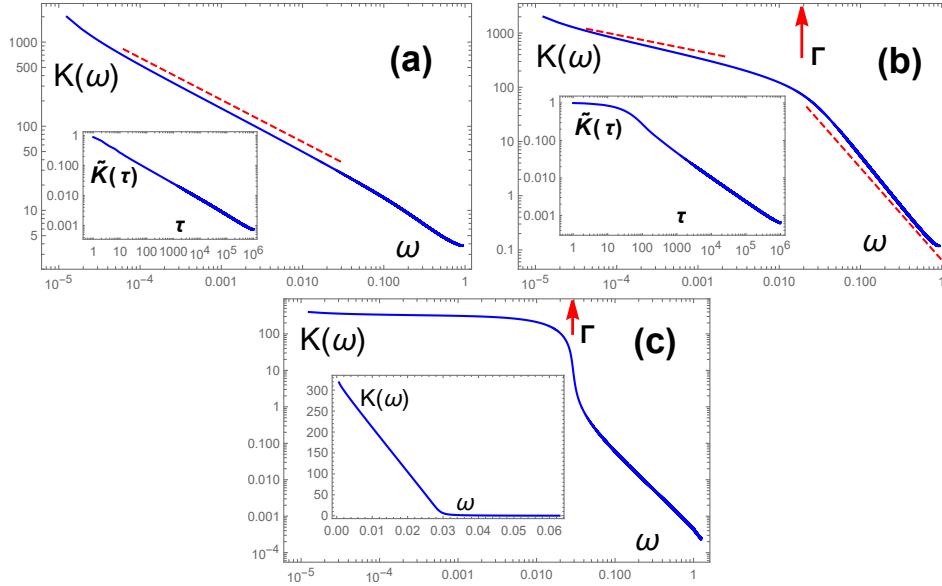


Figure 7: (Color online) The model LDoS correlation function computed exactly from Eqs.(16),(26) for: (a) a random Cantor set with $D = D_s = 0.5$, $N = 10^6$; (b) a mini-band with the Cantor set inside, $D = 0.5$, $D_s = 0.7$, $N = 10^6$; a mini-band with the dense spectrum inside, $D = 2/3$, $D_s = 1.5$, $N = 10^6$. The red dashed lines represent the power-laws, Eqs.(45),(44), expected at $N \rightarrow \infty$. Insets: (a) a power-law survival probability $\tilde{K}(\tau)$; (b) a slow dynamics of survival probability $\tilde{K}(\tau)$ at $\tau < 1/\Gamma$ and a power-law tail; (c) a quasi-linear behavior of $K(\omega)$ for $\delta < \omega < \Gamma$.

Concluding this section we would like to emphasize that in general, the exponent D in the definition of the number of levels in the local spectrum:

$$M \equiv N^D < N^{D_s}, \quad (D < D_s), \quad (48)$$

may depend on the way the discrimination of states is implemented and on the type of the local measure. In a particular case when the local measure

is $K(\omega)$ we have $D = D_2$ but for a generic local measure in a multifractal phase one may have a different $0 < D < 1$ which depends on the spectrum of multifractal dimensions D_q .

If $D < D_s$, a special type of the local singular-continuous spectrum, *the isolated mini-band*, emerges. For $D < D_s < 1$ the levels inside a mini-band form a random Cantor set with a hierarchical structure of higher-order mini-bands (see Fig.6(a)), while at $D_s > 1$ the spectrum inside a mini-band is dense (see Fig.6(d)). At $D_s = 1$ a special case of non-hierarchical and not completely dense spectrum (the *sub-dense* spectrum) shown in Fig.6(b) emerges inside a mini-band.

Note that the case $D_s < D \leq 1$ in Eq.(16) is inconsistent with the assumption that the typical level spacing δ_{typ} in the local spectrum is the same as in the global one $\delta_{\text{typ}} \sim \delta$. Indeed, with this assumption the total local spectral band-width is given by Eq.(47): $W_{\text{local}} \sim N^{\frac{D}{D_s}-1}$. By the discrimination procedure that eliminates levels from the global spectrum in order to obtain a local one, it must be equal or smaller than the total global spectral band-width $W_{\text{glob}} = 1$. This leaves only two options $D = D_s$ (random Cantor set) or $D < D_s$ (isolated mini-band). For the same reason the case $D = D_s = 1$ is marginally inconsistent with the above assumption, since in this case $W_{\text{loc}} \sim \ln(N) > 1$.

7. Hierarchy of mini-bands

As it is shown in Fig.4 and Fig.6(a) the regular and a random Cantor set can be considered as a *hierarchy of mini-bands*.

By a hierarchy of mini-bands we understand a spectrum such that at each of progressively decreasing scales Δ_i ($i = 1, 2, 3, \dots$) one finds a mini-band, i.e a set of consecutive levels obeying the following conditions (see Fig.8):

- *all* the spacings between them are smaller than Δ_i
- their total sum, the width of a mini-band $E_{mb}^{(i)}$, obeys $E_{mb}^{(i)} \leq \Delta_i$,
- the spacings on the right and on the left of a mini-band $s_{>}^{(i)}$ and $s_{<}^{(i)}$ obey the inequality $\min\{s_{>}^{(i)}, s_{<}^{(i)}\} \geq \Delta_i$.

Indeed, one can easily see that the regular Cantor set is such a hierarchy of mini-bands at *any* legitimate scale $\Delta_m = 3^{-m}$ bounded only by the minimal scale $\Delta = \delta$ from below and by the total spectral band-width 1 from above.

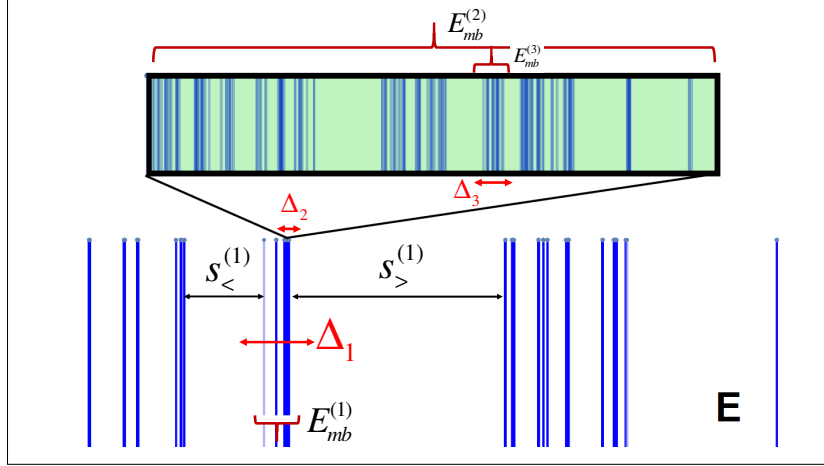


Figure 8: (Color online) A hierarchy of mini-bands. At each scale Δ_i ($i = 1, 2, 3, \dots$) one can identify a mini-band of the width $E_{mb}^{(i)}$ such that $E_{mb}^{(i)} \leq \Delta_i$ and the spacings $s_{>}^{(i)}, s_{<}^{(i)}$ on the right and on the left of the mini-band obey $\min\{s_{>}^{(i)}, s_{<}^{(i)}\} \geq \Delta_i$. A mini-band that at a scale Δ_1 looks like a single level at a scale Δ_2 (after a zoom) appears to be a mini-band containing yet a narrower mini-band at a scale Δ_3 .

Indeed, at the scale $\Delta_1 = 1/3$ the width of the two mini-bands $[0, 1/3]$ and $[2/3, 1]$ with the maximal spacing inside them $1/9 < \Delta_1$, are equal to Δ_1 ; at the next scale $\Delta_2 = 1/9$ one has 4 mini-bands of the width $\Delta_2 = 1/9$ with the maximal spacing $1/27 < \Delta_2$ and so on. Notice that the width of a mini-band at each scale Δ_i is equal to Δ_i . The same property (by the order of magnitude) has a random Cantor set (see Fig.6(a) and corresponding figure captions).

However, the hierarchy of mini-bands is not necessarily extended throughout the entire local spectrum. It may terminate from below prior to reaching $\Delta = \delta$. This happens if below some scale Δ_{\min} the local spectrum is dense, i.e. $\delta_{\text{av}} \sim \delta_{\text{typ}} \sim \delta$ (see Fig.9(b),(d)). It can also terminate from above at $\Delta_{\max} < 1$ if a mini-band of the width $\Gamma \sim \Delta_{\max}$ is isolated or if the gaps greater than Δ_{\max} *between the mini-bands* are all of the same order (see Fig.9((a),(c)). In particular, an isolated mini-band of Fig.3 with the dense

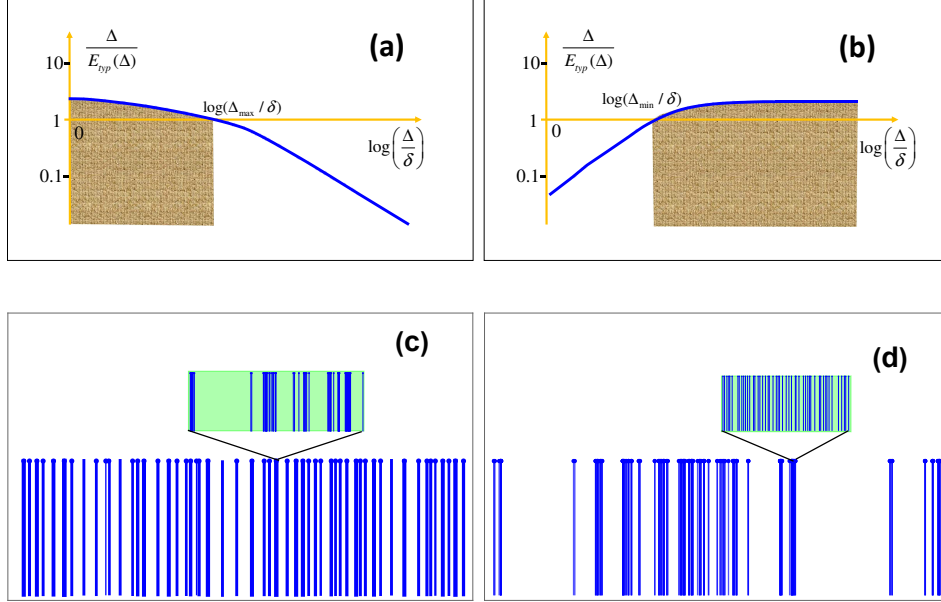


Figure 9: (Color online) More complicated local spectra. Fractality at small scales $\Delta < \Delta_{\max}$ and a non-hierarchical set of mini-bands at large scales $\Delta > \Delta_{\max}$ [(a), (c)]. A dense spectrum at small scales $\Delta < \Delta_{\min}$ and a hierarchical set of mini-bands at large scales $\Delta > \Delta_{\min}$ [(b), (d)]. The region of a hierarchical spectrum in (a) and (b) is shown by a texture.

spectrum inside realized in the Rosenzweig-Porter RMT, does not meet the above criteria of a hierarchy at any scale Δ , as in this case $\Delta_{\min} = \Delta_{\max} = \Gamma$.

In order to be able to describe such more complicated than a simple Cantor set cases we present the above conditions for the hierarchy of mini-bands in a form of a mathematical expression in terms of an *arbitrary* i.i.d. spacing distribution $P(s)$.

7.1. Criterion for existence of a hierarchy of mini-bands

In this section we derive a quantitative criterion of existence of a hierarchy of mini-bands and compute Δ_{\min} and Δ_{\max} for an arbitrary distribution $P(s)$ of independent identically distributed local spacings. We start by the expression for the probability for a string of n consecutive levels to obey the following conditions:

- all $(n-1)$ independently fluctuating spacings between them are smaller

than some Δ ,

- the spacing $s_>$ between the last level in a string and its nearest neighbor on the right is greater or equal than Δ .³

This probability is given by:

$$p_\Delta(n) = Q(1 - Q)^{n-1} \approx Q e^{-nQ}, \quad (49)$$

where $Q \ll 1$ is the probability for a *given* spacing to be greater than Δ :

$$Q \equiv Q(\Delta) = \int_\Delta^1 P(s) ds. \quad (50)$$

Now let us define the conditional probability $\mathcal{P}(E|n)$ that the string of n levels has a width E :

$$\mathcal{P}(E|n) = \prod_{k=1}^{n-1} \int ds_k P(s_k) \delta\left(\sum_{i=1}^{n-1} s_i - E\right). \quad (51)$$

For independently fluctuating spacings s_k this probability distribution function (PDF) is easy to calculate in terms of its (simple) Laplace transform:

$$\tilde{\mathcal{P}}(t|n) = \int_0^\infty \mathcal{P}(E|n) e^{-tE} = [g(t)]^{n-1}, \quad (52)$$

where $g(t)$ is defined by Eq.(27).

The PDF $P_\Delta(E)$ of the width E of a string of n levels with all spacings $s_i < \Delta$ separated from the rest of the spectrum by two gaps of the size larger than (or equal to) Δ is then given by:

$$P_\Delta(E) = \sum_{n=1}^M \mathcal{P}(E|n) p_\Delta(n). \quad (53)$$

³There is no need to impose the condition that the spacing $s_<$ between the first level in a string and its nearest neighbor on the left is greater or equal than Δ . This condition is automatically fulfilled, as the neighboring string on the left must have a gap $s'_> = s_<$ which is greater than Δ .

Now we impose the last and the most important condition to be fulfilled for such a string of n levels to be a mini-band. It is the condition that the *typical* width of the string $E_{\text{typ}}(\Delta)$ is smaller than or equal to Δ :

$$E_{\text{typ}}(\Delta) = \exp \left[\int \ln(E) P_{\Delta}(E) dE \right] \lesssim \Delta. \quad (54)$$

Eq.(54) is one of the principal results of this paper. Together with Eqs.(49)-(53) it defines the region where the hierarchy of mini-bands, or the fractality of local spectrum, is present (see Fig.9). The boundaries Δ_{min} and Δ_{max} of this region are given by the solutions for Δ of the *equation* at an equality sign in Eq.(54).

7.2. Examples of a random Cantor set and the dense and sub-dense spectrum

In order to test our approach we compute in Appendix A the typical width of a mini-band $E_{\text{typ}}(\Delta)$ for the case of a power-law $P(s)$, Eq.(16), and show that for $\Delta \gg \delta$:

$$\frac{\Delta}{E_{\text{typ}}(\Delta)} \sim \begin{cases} 1, & \text{for a random Cantor set } D = D_s < 1 \\ \ln^{-1} \left(\frac{\Delta}{\delta} \right) \ll 1, & \text{for a sub-dense spectrum } D = D_s = 1 \\ (\delta/\Delta)^{D_s-1} \ll 1, & \text{for a dense spectrum } D = 1, D_s > 1 \end{cases} \quad (55)$$

As expected, this calculation showed that only the case of a random Cantor set obeys the criterion of fractality, Eq.(54), while the dense and sub-dense spectra violate it. More complicated examples are illustrated in Fig.9

8. Conclusion

The goal of this paper was to explain in simple terms what does the singular-continuous spectrum mean from the physics point of view. In contrast to the mathematical literature where a continuous limit is always assumed, we consider a discrete system of a finite (but large) number of degrees of freedom N assuming a coarse-graining at small distances (e.g. a lattice with a fixed lattice constant $a = 1$) and taking the limit $1/N \rightarrow 0$ only in the final results.

Starting from a regular textbook Cantor set we increased complexity of the model of singular continuous spectrum by considering first a *random* Cantor set and then generalizing it to the *hierarchy of mini-bands*.

The key ingredient of such constructions was the power-law tailed distribution function $P(s)$ of independent identically distributed spacings between

levels seen in the *local density of states* (LDoS). We have shown how such a tailed distribution emerges in the limit $N \rightarrow \infty$ as the result of discrimination that discards states with the amplitude in the observation point smaller than N^{-1} . This mechanism explains a qualitative difference between the fractal local spectrum (seen in LDoS) and the dense global spectrum (seen in the global DoS) in the non-ergodic extended phases of disordered systems.

We have demonstrated that within our simple model there are two classes of the local singular-continuous spectra in the non-ergodic extended phases: (i) the random Cantor set and (ii) the isolated mini-band. They are realized in the critical Power-Law Banded Random Matrices (CPLBRM) [21, 42, 43, 44] and in the Rosenzweig-Porter (RP) RMT [3, 4, 7], respectively. Using the model of independent identically distributed (i.i.d.) local level spacings we reproduced in both cases (i) and (ii) the correlation functions $K(\omega)$ of the local densities of states which was previously known from the analytical and numerical studies [42, 43, 44, 3, 45, 36, 23]. This confirms our conjecture that the simplified picture of i.i.d. local level spacings with the power-law distribution is a correct qualitative description of the above two limiting cases and that the CPLBRM and RP are characterized by the local singular continuous spectrum of the type of the Cantor set and of the type of the isolated mini-band, respectively.

Our model is characterized⁴ by two fractal dimensions: the eigenfunction fractal dimension D that describes the number of states N^D (with the typical amplitude of wave function $|\psi|^2 \sim N^{-D}$) seen in the local spectrum after the discrimination, and the spectral fractal dimension D_s which determines the power-law distribution of local spacing, Eq.(16). Depending on the relationship between them, different types of local spectra emerge from our model. All our results are summarized in Table 1.

Three of these cases shown in the rows 1 [Fig.6(a)], 2 [Fig.6(c)] and 5 [Fig.6(d)] have well-known Hamiltonian realizations: the multifractal states of the critical Power-Law Banded Random Matrices and those at the critical points of the Anderson localization transitions (row 1), the ergodic states of the Wigner-Dyson RMT (row 2) and the fractal states in the Gaussian Rosenzweig-Porter RMT (row 5 with $D_s = 1 + \epsilon$, $\epsilon \rightarrow 0$). We are confident that the cases presented in row 3 [a mini-band with a random Cantor

⁴besides the typical level spacing $\delta = 1/N$ which in extended phases is supposed to be of the same order both in the global and in the local spectrum

Table 1: **The character of local spectrum, $K(\omega)$ and width of a mini-band Γ**

<i>condition</i>	<i>local spectrum</i>	$K(\omega)$	Γ
$D = D_s < 1$	random Cantor set	$\omega^{-(1-D_s)}, \delta < \omega < 1$	1
$D = 1, D_s > 1$	dense set of levels	~ 1	1
$D < D_s < 1$	isolated mini-band random Cantor set inside	$\Gamma^{-D_s} \omega^{-(1-D_s)}, \delta < \omega < \Gamma,$ $\Gamma^{D_s} \omega^{-(1+D_s)}, \Gamma < \omega < 1$	$N^{-(1-D/D_s)}$
$D < D_s = 1$	isolated mini-band sub-dense spectrum inside	$\Gamma^{-1} \ln(N^D) \ln^{-1}(\omega/\delta), \delta < \omega < \Gamma,$ $\Gamma \omega^{-2} \ln^{-1}(N^D), \Gamma < \omega < 1$	$N^{-(1-D)} \ln(N^D)$
$D < 1, D_s > 1$	isolated mini-band dense spectrum inside	$\Gamma^{-1}, \delta < \omega < \Gamma$ $\Gamma^{-1}(\Gamma/\omega)^{1+D_s} N^{-D(D_s-1)}, \Gamma < \omega < 1$	$N^{-(1-D)}$
$D = D_s = 1$ $D_s < D \leq 1$	inconsistent with $\delta_{\text{typ}} \sim \delta$		

set, Fig.6(a), inside] and row 4 [a mini-band with a sub-dense spectrum of Fig.6(b) inside] also have their Hamiltonian realizations. To find them is an interesting problem of both fundamental and applied significance ⁵.

It is important that in all the cases when the eigenfunction fractal dimension $D < 1$ (non-ergodic extended states) our model gives a singular continuous spectrum of the type of a random Cantor set or an isolated mini-band. An absolutely continuous local spectrum of Fig.6(a) emerges only if $D = 1$.

In the limit $N \rightarrow \infty$ we obtain from Table 1:

$$\lim_{N \rightarrow \infty} K(\omega) \sim \begin{cases} \omega^{-1+D_s}, & \text{for a random Cantor set} \\ \delta(\omega), & \text{for an isolated mini band} \\ 1, & \text{for an absolutely continuous spectrum} \end{cases} \quad (56)$$

Eq.(56) expresses a very general important result: The LDoS correlation function in the limit $N \rightarrow \infty$ is a measure that distinguishes between the absolutely continuous and the singular continuous spectra in delocalized phases. While the former results in a finite limit for $\lim_{N \rightarrow \infty} K(\omega)$ at $\omega \rightarrow 0$, the latter implies the singularity at $\omega = 0$. Furthermore, the type of the singularity unambiguously identifies the type of a singular-continuous spectrum. For the localized eigenstates the typical level spacing in the local spectrum is finite in $N \rightarrow \infty$ limit and, hence, $K(\omega \rightarrow 0) \rightarrow 0$ in this limit.

Extending the simple picture described above to an arbitrary distribution of local level spacing, we formulated a general criterion, Eq.(54), of fractality

⁵The two cases presented in the row 6 are inconsistent with the assumption that the typical level spacing in the local spectrum $\delta_{\text{typ}} \sim \delta$ is of the same order as that in the global one (see footnote ¹).

of local spectra and tested it by considering the examples of the random Cantor set, the isolated mini-band and the dense spectrum. The criterion Eq.(54) is one of the main results of the paper which can be used to characterize more complicated local spectra in the non-ergodic extended phases.

Acknowledgment. We are grateful to E. Bogomolny, M. V. Feigel'man, I. M. Khaymovich, P. Nosov, A. Scardicchio and M. Zirnbauer for stimulating discussions and useful comments on the manuscript. V.E.K. also appreciates collaboration with L. B. Ioffe and M. Pino during the work on Ref.[11] where some preliminary results of this paper were communicated. The support from the Google Quantum Research Award ‘‘Ergodicity Breaking in Quantum Many-Body Systems’’ (V.E.K.) is gratefully acknowledged.

Appendix A. A test of Eq.(54) for a power-law $P(s)$ in Eq.(16)

Appendix A.1. Example of a random Cantor set

In order to illustrate a general formalism Eqs.(49)-(54) we consider an example of a random Cantor set with $D = D_s < 1$, where D is defined in Eq.(48).

Consider Eq.(52) in the limit $n \gg 1$ with $g(t)$ from Eq.(31):

$$[g(t)]^{n-1} \approx \exp[-n(t\delta)^{D_s}]. \quad (\text{A.1})$$

Then the PDF $\mathcal{P}(E|n)$ is given by the Laplace transform:

$$\mathcal{P}(E|n) = \int_B \exp[-n(t\delta)^{D_s} + Et] dt, \quad (\text{A.2})$$

where the integral runs over the Bromwich contour $t \in (-i\infty + 0, i\infty + 0)$ as customary for the inverse Laplace transform ⁶.

Next we do summation over n according to Eqs.(53),(49):

$$P_\Delta(E) = Q \int_B \frac{e^{Et}}{Q + (t\delta)^{D_s}} \frac{dt}{2\pi i}, \quad (\text{A.3})$$

using the smallness of Q and $t\delta$ to approximate $1 - e^{-(Q+(t\delta)^{D_s})} \approx Q + (t\delta)^{D_s}$ and large values of $M(Q+(t\delta)^{D_s}) \gg 1$ to extend summation over n to infinity.

⁶As a matter of fact, Eq.(A.2) defines a PDF of the *Levy α -stable distribution* with $\alpha = D_s$.

Integrating e^{Et} over the Bromvich contour first to obtain $\delta(t)$, one can easily check that the distribution function $P_\Delta(E)$ is correctly normalized.

The Bromvich contour in Eq.(A.3) can be deformed to go along the branch cut $(-\infty - i0, 0) \cup (0, -\infty + 0)$. Then switching $t \rightarrow -t$ we obtain:

$$P_\Delta(E) = \frac{\sin(\pi D_s)}{\pi} Q \int_0^\infty dt e^{-Et} \frac{(t\delta)^{D_s}}{Q^2 + (t\delta)^{2D_s} + 2Q(t\delta)^{D_s} \cos(\pi D_s)}. \quad (\text{A.4})$$

The integral in this expression is controlled by a parameter E/E_* , where:

$$E_* = \frac{\delta}{Q^{\frac{1}{D_s}}}, \quad (\text{A.5})$$

and in the limiting cases $E \ll E_*$ and $E \gg E_*$ it is equal to:

$$P_\Delta(E) = \frac{\sin\left(\frac{\pi D_s}{2}\right)}{\pi} \begin{cases} \frac{\Gamma(1-D_s)}{E} \left(\frac{E}{E_*}\right)^{D_s}, & (E \ll E_*) \\ \frac{\Gamma(1+D_s)}{E} \left(\frac{E_*}{E}\right)^{D_s}, & (E \gg E_*) \end{cases} \quad (\text{A.6})$$

The sketch of the distribution function $P_\Delta(E)$ and the corresponding spacing distribution is shown in Fig.A.10. As the integral of $P_\Delta(E)$ over $E < E_*$ (the normalization integral) is dominated by the upper limit $E \sim E_*$, and the corresponding integral over $E > E_*$ is dominated by the lower limit $E \sim E_*$, the main contribution to the normalization integral of $P_\Delta(E)$ comes from the vicinity of $E \approx E_*$ given by Eq.(A.5). By definition E_* is the typical width $E_{\text{typ}}(\Delta)$ of a mini-band at a scale Δ .

The last step is to substitute $Q = Q(\Delta)$ in Eq.(A.5). For the local spacing distribution function $P(s)$, Eq.(16), one readily finds:

$$Q(\Delta) \sim \left(\frac{\delta}{\Delta}\right)^{D_s}, \quad (\text{A.7})$$

so that

$$E_* = E_{\text{typ}}(\Delta) \sim \Delta. \quad (\text{A.8})$$

We conclude, therefore, that for the random Cantor set, like for its regular counterpart, the typical width of a mini-band at a scale Δ is of the order of Δ . This saturates the criterion, Eq.(54) which is therefore fulfilled for *any* $\Delta > \delta$. This result was expected but it serves as an important test for the consistency of the formalism Eqs.(49)-(54) developed in Section 7. Since the random Cantor set is considered as an archetypical example of a fractal spectrum, the fulfillment of the criterion Eq.(54) in general signals on the fractality of the local spectrum.

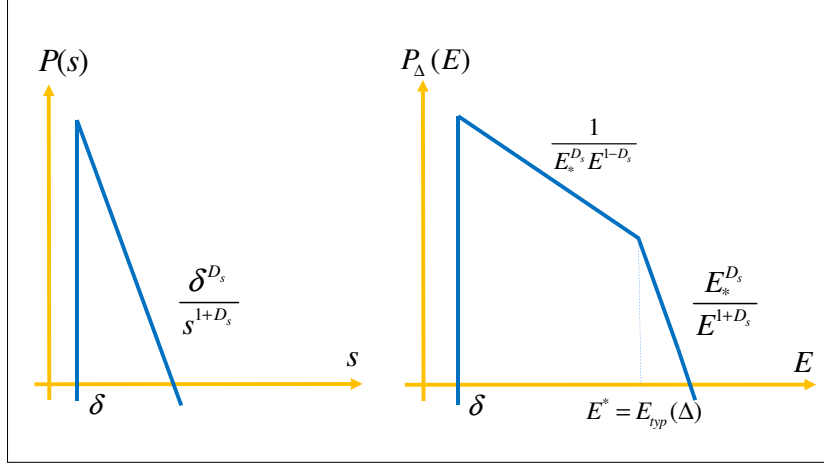


Figure A.10: (Color online) The distribution of local spacings in the log-log coordinates (Left panel) and the corresponding distribution of the width E of a mini-gap at a scale Δ (Right panel) for the random Cantor set. The main contribution to the normalization integral of $P_\Delta(E)$ is given by $E_* = E_{\text{typ}}(\Delta)$.

Appendix A.2. Example of an isolated mini-band

Now we consider the case $D < D_s$ in Eqs.(48),(16) which corresponds to an isolated mini-band. First of all we note that Eq.(A.3) is only valid if one can neglect the boundary term in the summation of geometric series. This necessarily requires $MQ = N^D Q \gg 1$, which by the virtue of Eq.(A.7) implies:

$$\Delta \ll \Delta_{\text{max}} = \Gamma \sim \begin{cases} N^{-1+\frac{D}{D_s}}, & D_s < 1 \\ N^{-1+D}, & D_s \geq 1 \end{cases}. \quad (\text{A.9})$$

Within this restriction let us consider the character of spectrum *inside a mini-band* of the width Γ . If $D_s < 1$ the results of the previous subsection [Eq.(35) with $M \sim N^D$] show that the spectrum inside a mini-band is a random Cantor set with the hierarchy of mini-bands.

If $D < 1$ and $D_s = 1$ we have using Eq.(32):

$$P_\Delta(E) \approx \frac{Q}{2} \int_0^\infty dt e^{-Et} \frac{(t\delta)}{(Q - (t\delta) \ln(t\delta))^2} = \begin{cases} \frac{Q}{2\delta \ln^2(E/\delta)}, & \delta \ll E \ll E_* \\ \frac{\delta}{2QE^2}, & \Gamma \gg E \gg E_* \end{cases}, \quad (\text{A.10})$$

where $Q = \delta/\Delta$ and

$$E_* = \Delta \ln(\Delta/\delta). \quad (\text{A.11})$$

As in the previous subsection, one can see that the main contribution to the normalization integral for $P_\Delta(E)$ is given by $E \approx E_*$, so that $E_{\text{typ}}(\Delta) = E_*$. Therefore,

$$E_{\text{typ}}(\Delta) > \Delta \quad (\text{A.12})$$

in the entire region $\delta \ll \Delta < \Gamma$. The failure to fulfill the criterion Eq.(54) implies that for $D < D_s = 1$ the spectrum inside the mini-band does not have a hierarchical structure. At the same time it has large gaps and thus is not completely dense. The similar spectrum appears in the entire band for the case $D = D_s = 1$ (see Fig.6(b)).

Finally, let us consider the case $D < 1$ but $2 > D_s > 1$. In this case it follows from Eq.(33) that:

$$P_\Delta(E) \approx Q \int_B \frac{e^{Et}}{Q + c_1(t\delta) + c_2(t\delta)^{D_s}} \frac{dt}{2\pi i}, \quad (\text{A.13})$$

where c_1 and c_2 are coefficients of order 1.

The Bromwich contour B of integration can be deformed to encircle the cut $(-\infty, 0)$. Then at $E/\delta \gg 1$ the main contribution comes from $t\delta \ll 1$, so that the term $c_2(t\delta)^{D_s}$ is a correction. The leading t -dependence leads to a pole at $c_1 t\delta = Q$ with the result:

$$P_\Delta(E)|_{\text{pole}} = \frac{c_1}{E_*} e^{-(E/E_*)} \quad (\text{A.14})$$

where

$$E_* = \frac{c_1 \delta}{Q}. \quad (\text{A.15})$$

This pole contribution is almost constant for $E \ll E_*$ and it is exponentially small at $E \gg E_*$. In this latter region one should take into account a correction $c_2(t\delta)^{D_s}$ which takes different values at $t = -x+i0$ and $t = -x-i0$, ($x > 0$):

$$P_\Delta(E)|_{\text{corr}} = \frac{c_2 \sin(\pi D_s)}{\pi} \int_0^\infty dx e^{-Ex} \frac{(x\delta)^{D_s}}{Q} \quad (\text{A.16})$$

Collecting the results at $E \ll E_*$ and $E \gg E_*$ we finally obtain:

$$P_\Delta(E) \sim \begin{cases} \frac{e^{-E/E_*}}{E_*}, & \delta \ll E \ll E_* \ln[c(E_*/\delta)^{D_s-1}] \\ \left(\frac{\delta}{E}\right)^{D_s+1} \frac{E_*}{\delta^2}, & \Gamma \gg E \gg E_* \ln[c(E_*/\delta)^{D_s-1}] \end{cases}, \quad (\text{A.17})$$

where $c \sim 1$.

One can see again that the main contribution to the normalization integral comes from $E \sim E_*$. So, from Eqs.(A.7),(A.15) we obtain:

$$E_{\text{typ}}(\Delta) \sim E_* \sim \Delta \left(\frac{\Delta}{\delta}\right)^{D_s-1} \gg \Delta, \quad (\text{A.18})$$

for all $\Delta \gg \delta$. This result remains valid for all $D_s > 1$.

In this case the length of the string of levels with all spacing between them smaller than Δ is larger by a polynomially large parameter $(\Delta/\delta)^{D_s-1}$ than the gaps between such strings. This makes large gaps extremely rare which means dense typical local spectrum inside a mini-gap at $D < 1$ and that in the entire spectral band for $D = 1$ (see Fig.6(c)).

Appendix A.3. Example of a dense spectrum

This case is easy to obtain from the results of the previous subsection at $D = 1$ and $D_s > 1$. The only modification needed is to replace $\Delta_{\text{max}} = \Gamma$ given by Eq.(A.9) by the entire band-width $\Delta_{\text{max}} = \Gamma = 1$. After this modification Eq.(A.17) remains valid in the entire region $\delta < E < 1$, and Eq.(A.18) gives:

$$\frac{\Delta}{E_{\text{typ}}(\Delta)} \sim \left(\frac{\delta}{\Delta}\right)^{D_s-1} \ll 1. \quad (\text{A.19})$$

Thus the criterion of fractality of local spectrum, Eq.(54), is strongly violated as it should be for the dense spectrum.

References

- [1] G. Biroli, A. Ribeiro-Teixeira, and M. Tarzia. Difference between level statistics, ergodicity and localization transitions on the bethe lattice. 2012.
- [2] A. De Luca, B. L. Altshuler, V. E. Kravtsov, and A. Scardicchio. Anderson localization on the Bethe lattice: Nonergodicity of extended states. *Phys. Rev. Lett.*, 113(4):046806, 2014.

- [3] V. E. Kravtsov, I. M. Khaymovich, E. Cuevas, and M. Amini. A random matrix model with localization and ergodic transitions. *New J. Phys.*, 17:122002, 2015.
- [4] D. Facchetti, P. Vivo, and G. Biroli. From non-ergodic eigenvectors to local resolvent statistics and back: A random matrix perspective. *EPL (Europhysics Letters)*, 115:47003, 2016.
- [5] Per von Soosten and Simone Warzel. Non-ergodic delocalization in the Rosenzweig–Porter model. *Letters in Mathematical Physics*, pages 1–18, 2018.
- [6] V.E.Kravtsov, B.L.Altshuler, and L.B.Ioffe. Non-ergodic delocalized phase in Anderson model on Bethe lattice and regular graph. *Annals of Physics*, 389:148–191, 2018.
- [7] I. M. Khaymovich, V. E. Kravtsov, B. L. Altshuler, and L. B. Ioffe. Fragile ergodic phases in logarithmically-normal Rosenzweig–Porter model. *Phys. Rev. Research*, 2:043346, 2020.
- [8] I. García-Mata, O. Giraud, B. Georgeot, J. Martin, R. Dubertrand, and G. Lemarié. Scaling theory of the Anderson transition in random graphs: ergodicity and universality. *Phys. Rev. Lett.*, 118:166801, Apr 2017.
- [9] K. S. Tikhonov and A. D. Mirlin. Statistics of eigenstates near the localization transition on random regular graphs. *Phys. Rev. B.*, 99:024202, 2019.
- [10] A. K. Das and A. Ghosh. Nonergodic extended states in the β ensemble. *Phys. Rev. E*, 105:054121, 2022.
- [11] M. Pino, V. E. Kravtsov, B. L. Altshuler, and L. B. Ioffe. Multifractal metal in a disordered Josephson junctions array. *Phys. Rev. B*, 96:214205, 2017.
- [12] N Macé, F Alet, and N Lafflorencie. Multifractal scalings across the many-body localization transition. *Phys. Rev. Lett.*, 123:180601, 2019.
- [13] D. J. Luitz, I. M. Khaymovich, and Y. Bar Lev. Multifractality and its role in anomalous transport in the disordered xxz spin-chain. *SciPost Phys*, Core 2:006, 2020.

- [14] A. Bäcker, M. Haque, and I. M. Khaymovich. Multifractal dimensions for random matrices, chaotic quantum maps, and many-body systems. *Phys. Rev. E*, 100(3):032117, 2019.
- [15] K. S. Tikhonov and A. D. Mirlin. From Anderson localization on random regular graphs to many-body localization. *Annals of Physics*, 435:168525, 2021.
- [16] G. De Tomasi, I. M. Khaymovich, F. Pollmann, and S. Warzel. Rare thermal bubbles at the many-body localization transition from the Fock space point of view. *Phys. Rev. B.*, 104:024202, 2021.
- [17] V. R. Motamarri, A. S. Gorsky, and I. M. Khaymovich. Localization and fractality in disordered russian doll model. *SciPostPhysics*, 13:117, 2022.
- [18] A. De Luca and A. Scardicchio. Ergodicity breaking in a model showing many-body localization. *Europhys. Lett.*, 101:37003, 2013.
- [19] M. Tarzia. Many-body localization transition in hilbert space. *Phys. Rev. B*, 102:014208, 2020.
- [20] Ferdinand Evers and Alexander Mirlin. Anderson transitions. *Rev. Mod. Phys.*, 80:1355, 2008.
- [21] A. D. Mirlin, Y. V. Fyodorov, F.-M. Dittes, J. Quezada, and T. H. Seligman. Transition from localized to extended eigenstates in the ensemble of power-law random banded matrices. *Phys. Rev. E*, 54:3221, 1996.
- [22] N. Rosenzweig and C. E. Porter. "repulsion of energy levels" in complex atomic spectra. *Phys. Rev. B*, 120:1698, 1960.
- [23] C. Monthus. Multifractality of eigenstates in the delocalized non-ergodic phase of some random matrix models: Wigner-Weisskopf approach. *J. Phys. A: Math. Theor.*, 50(29):295101, jun 2017.
- [24] Giuseppe de Tomasi, Moshen Amini, Soumya Bera, Ivan M. Khaymovich, and Vladimir E. Kravtsov. Survival probability in Generalized Rosenzweig-Porter random matrix ensemble. *SciPost Phys.*, 6:014, 2019.
- [25] I M Khaymovich and V E Kravtsov. Dynamical phases in a "multifractal" Rosenzweig-Porter model. *SciPost Phys.*, 11:045, 2021.

- [26] S. Bera, G. De Tomasi, I. M. Khaymovich, and A. Scardicchio. Return probability for the Anderson model on the random regular graph. *Phys. Rev. B*, 98:134205, 2018.
- [27] G. De Tomasi, S. Bera, A. Scardicchio, and I. M. Khaymovich. Subdiffusion in the Anderson model on random regular graph. *Phys. Rev. B*, 101:100201, 2019.
- [28] Y. Bar Lev, G. Cohen, and D. R. Reichman. Absence of Diffusion in an Interacting System of Spinless Fermions on a One-Dimensional Disordered Lattice. *Phys. Rev. Lett.*, 114:100601, 2015.
- [29] K. Agarwal, S. Gopalakrishnan, M. Knap, M. Müller, and E. Demler. Anomalous Diffusion and Griffiths Effects Near the Many-Body Localization Transition. *Phys. Rev. Lett.*, 114:160401, 2015.
- [30] D. J. Luitz, N. Laflorencie, and F. Alet. Extended slow dynamical regime close to the many-body localization transition. *Phys. Rev. B*, 93:060201, 2016.
- [31] D. J. Luitz and Y. Bar Lev. Anomalous thermalization in ergodic systems. *Phys. Rev. Lett.*, 117:170404, 2016.
- [32] M. Schulz, S. R. Taylor, C. A. Hooley, and A. Scardicchio. Energy transport in a disordered spin chain with broken $u(1)$ symmetry: Diffusion, subdiffusion, and many-body localization. *Phys. Rev. B*, 98:180201, 2018.
- [33] T. L. M. Lezama, S. Bera, and J. H. Bardarson. Apparent slow dynamics in the ergodic phase of a driven many-body localized system without extensive conserved quantities. *Phys. Rev. B*, 99:161106, 2019.
- [34] N. Dunford and J.T. Schwartz. *Linear Operators, Part II: Spectral Theory*. Interscience, New York, 1963.
- [35] M. L. Mehta. *Random matrices*. Elsevier, 2004.
- [36] Cécile Monthus. Statistical properties of the Green function in finite size for Anderson localization models with multifractal eigenvectors. *Journal of Physics A: Mathematical and Theoretical*, 50(11):115002, feb 2017.

- [37] R. Berkovits. Super-Poissonian behavior of the Rosenzweig-Porter model in the nonergodic extended regime. *Phys. Rev. B*, 102:165140, 2020.
- [38] M. A. Skvortsov, M. Amini, and V. E. Kravtsov. Sensitivity of (multi)fractal eigenstates to a perturbation of the Hamiltonian. *Phys. Rev. B*, 106:054208, 2022.
- [39] J. T. Chalker and G. J. Daniel. Scaling, diffusion, and the integer quantized hall effect. *Phys. Rev. Lett.*, 61:593, 1988.
- [40] J. T. Chalker. Scaling and eigenfunction correlations near a mobility edge. *Physica A: Statistical Mechanics and its Applications*, 167:253, 1990.
- [41] A. B. Harris. Effect of random defects on the critical behaviour of Ising models . *J. Phys. C: Solid State Physics*, 7(9):1671, 1974.
- [42] V. E. Kravtsov and K. A. Muttalib. New Class of Random Matrix Ensembles with Multifractal Eigenvectors. *Phys. Rev. Lett.*, 79:1913, 1997.
- [43] E. Cuevas and V. E. Kravtsov. Two-eigenfunction correlation in a multifractal metal and insulator. *Phys. Rev. B*, 76(235119), 2007.
- [44] V. E. Kravtsov, A. Ossipov, O. M. Yevtushenko, and E. Cuevas. Dynamical scaling for critical states: Validity of Chalker’s ansatz for strong fractality . *Phys. Rev. B*, 82:161102, 2010.
- [45] M. A. Skvortsov, M. Amini, and V. E. Kravtsov. Sensitivity of (multi) fractal eigenstates to a perturbation of the Hamiltonian. *Phys. Rev. B*, 106:054208, 2022.